

Crystal stability and optical properties of organic chain compounds

P. ŽUPANOVIĆ¹, A. BJELIŠ² and S. BARIŠIĆ²

¹ Department of Physics, Faculty of Science and Art, University of Split
Teslina 10, 21000 Split, Croatia

² Department of Physics, Faculty of Science, University of Zagreb
POB 162, 10001 Zagreb, Croatia

(received ; accepted)

PACS. 61.50Lt – Crystal binding; cohesive energy .

PACS. 61.66Hq – Organic compounds.

PACS. 78.30Jw – Organic solids, polymers.

Abstract. –

The solution to the long standing problem of the cohesion of organic chain compounds is proposed. We consider the tight-binding dielectric matrix with two electronic bands per chain, determine the corresponding hybridized collective modes, and show that three among them are considerably softened due to strong dipole-dipole and monopole-dipole interactions. By this we explain the unusual low frequency optical activity of TTF-TCNQ, including the observed 10meV anomaly. The softening of the modes also explains the cohesion of the mixed-stack lattice, the fractional charge transfer almost independent of the material, and the formation of the charged sheets in some compounds.

Ever since the discovery of the mixed stack organic chain compounds (OCCs), some twenty five years ago, two important questions remained open [1]. The first is the stability of their crystal structure, with a fractional charge transfer between the molecules of $n_a \approx 0.6$ electrons per molecule. Furthermore, in some lattices like TTF-TCNQ the equally charged (TTF or TCNQ) chains stack side by side, to form charged sheets, instead of alternating in both directions, as suggested by the simple Madelung argument. Such a simple alternation does occur in other lattices, like HMTTF-TCNQ, which, in spite of the radically different chain stacking, have similar n_a . Neither the fractional charge transfer nor the formation of charged sheets are expected within the standard ionic cohesion scheme which assumes the dominance of affinity-ionicity and electrostatic (Madelung) contributions. Besides, calculations of cohesion energy within this scheme suggest that almost 2 eV per donor-acceptor molecular pair is lacking. This "Madelung defect" [2] clearly signifies that the cohesion at a scale of few eVs has to be stabilized by some mechanism(s) beyond the standard ionic scheme. Although various suggestions [2]-[7] have been put forward, they have failed to explain all the aspects of the cohesion, mostly because they could not account for the Madelung defect.

On the other hand, Friedel [8] pointed out that the van der Waals interaction between the molecules favors the formation of charged sheets observed in TTF-TCNQ. In this model the intramolecular (interband) and the intermolecular (intraband) charge fluctuations are separated. Such separation however fails in the low frequency range in which TTF-TCNQ shows strong anomalies, observed in numerous microwave/infrared optical measurements [9]-[13] (fig.1).

The origin of these anomalies is the second puzzle of OCCs. E. g. in TTF-TCNQ the frequency of the anomaly at 10 meV [10, 11] is comparable to the value of the (pseudo)gap Δ_L produced by the $2k_F$ lattice instability at low temperatures ($T < 50K$). However the anomalies in fig.1 can not be related to this instability, since they persist at high temperatures, where the $2k_F$ lattice fluctuations are practically absent.

In this Letter we present a theory which for the first time treats interband (van der Waals) and intraband correlations on equal footing, and explains simultaneously the crystal stability and the optical anomalies of OCCs. We investigate a simple model with two orbitals per donor and acceptor molecule, i. e. two bands per molecular chain, the lower bands being partially filled. Applying the recently proposed tight-binding formalism for the dielectric matrix in the random phase approximation (RPA) [14], we determine the hybridized collective modes associated with the electron polarization processes, and the corresponding zero-point energy contributions to the cohesive energy. We show that the above unusual cohesive and optical properties are related through the presence of a soft interband collective mode and its hybridization with the intraband charge fluctuations.

In the tight-binding formalism [14] the matrix elements of the screened Coulomb interaction $\bar{V}(\mathbf{r}, \mathbf{r}')$ are represented in terms of interband and intraband polarization processes, and the corresponding system of RPA Dyson equations reads

$$\sum_{p_g} [\delta_{p_e p_g} - V_{p_e p_g}(\mathbf{q}) \Pi_{p_g}(\mathbf{q}, \omega)] \bar{V}_{p_g p_f}(\mathbf{q}, \omega) = V_{p_e p_f}(\mathbf{q}). \quad (1)$$

Here the matrix elements of the bare Coulomb interaction $V(\mathbf{r} - \mathbf{r}')$ are given by

$$V_{p_e p_f}(\mathbf{q}) = \sum_{\mathbf{R}} e^{i\mathbf{q}(\mathbf{R} + \mathbf{e} - \mathbf{f})} \int d\mathbf{r} \int d\mathbf{r}' \varphi_{l_e}^*(\mathbf{r} - \mathbf{R} - \mathbf{e}) \varphi_{n_f}^*(\mathbf{r}' - \mathbf{f}) V(\mathbf{r} - \mathbf{r}') \varphi_{l'_e}(\mathbf{r} - \mathbf{R} - \mathbf{e}) \varphi_{n'_f}(\mathbf{r}' - \mathbf{f}). \quad (2)$$

\mathbf{R} are lattice vectors, and \mathbf{e} and \mathbf{f} are positions of the molecules within the unit cell. The latter take values $\mathbf{0}$ and $\mathbf{a}/2$ for acceptor and donor molecules respectively, with $\mathbf{R} = N_a \mathbf{a} + N_c \mathbf{c}$ for TTF-TCNQ, and $\mathbf{R} = N_1(\mathbf{a}/2 + \mathbf{c}) + N_2(\mathbf{a}/2 - \mathbf{c})$ for HMTTF-TCNQ. Here $N_{a,c,1,2}$ are integers, and a simplified orthorombic symmetry with one donor and one acceptor chain per unit cell is assumed. The wave function $\varphi_{l_e}(\mathbf{r} - \mathbf{R} - \mathbf{e})$ in eq.2 is l_e -th orbital at the molecular site $\mathbf{R} + \mathbf{e}$, and $p_e \equiv (l_e, l'_e)$ stays for the one-electron transition between l_e and l'_e orbitals. We do not keep negligible contributions due to finite direct overlaps between orbitals from neighboring molecules. Having in mind the known electronic spectra of e. g. TCNQ [15] and TTF [16] molecules, we specify that the orbitals which form lower (partially filled) and upper (empty) bands have the same, A_g and B_{2u} , respective symmetries on both, acceptor and donor, sublattices. This means that the interband transitions on both families of chains are dipole active, with the dipole matrix elements $\mu_{a(d)}$ oriented along the chain direction \mathbf{b} . With the standard assumption that all products $\varphi_{l_e}^*(\mathbf{r}) \varphi_{l'_e}(\mathbf{r})$ are real, we get from eq.1 the

dielectric matrix

$$[\varepsilon] = \begin{bmatrix} 1 - V_{0_a 0_a} \Pi_{0_a} & -V_{0_a 0_d} \Pi_{0_d} & V_{0_a 1_a} \Pi_{1_a} & -V_{0_a 1_d} \Pi_{1_d} \\ -V_{0_d 0_a} \Pi_{0_a} & 1 - V_{0_d 0_d} \Pi_{0_d} & -V_{0_d 1_a} \Pi_{1_a} & -V_{0_d 1_d} \Pi_{1_d} \\ -V_{1_a 0_a} \Pi_{0_a} & -V_{1_a 0_d} \Pi_{0_d} & 1 - V_{1_a 1_a} \Pi_{1_a} & -V_{1_a 1_d} \Pi_{1_d} \\ -V_{1_d 0_a} \Pi_{0_a} & -V_{1_d 0_d} \Pi_{0_d} & -V_{1_d 1_a} \Pi_{1_a} & 1 - V_{1_d 1_d} \Pi_{1_d} \end{bmatrix} \quad (3)$$

for the microscopic response to the longitudinal electric field. Here indices $0_{a(d)}$ and $1_{a(d)}$ represent intraband and interband one-electron transitions on the acceptor (donor) chains, respectively. $\Pi_{0_{a(d)}}$ and $\Pi_{1_{a(d)}}$ are intraband and interband bubble polarization diagrams, and V 's are the corresponding matrix elements of eq. 2. Our main aim is to determine collective modes, i. e. zeros of the microscopic dielectric function $\varepsilon(\omega) = \det[\varepsilon]$, in the long wavelength limit $\mathbf{q} \rightarrow 0$. In this limit the intraband polarization diagrams are given by $\Pi_{0_{a(d)}}(\mathbf{q}, \omega) \approx (\mathbf{q} \cdot \mathbf{b})^2 \omega_{0_{a(d)}}^2 / 4\pi e^2 b^2 \omega^2$, while the interband polarization diagrams reduce to $\Pi_{1_{a(d)}}(\mathbf{q}, \omega) \approx 2n_{a(d)} E_{a(d)} / (\omega^2 - E_{a(d)}^2)$, after taking into account that the energy gaps on both types of chains, $E_{a(d)}$ ($\approx 3eVs$) [19], are considerably higher than the bandwidths ($\approx 0.5eVs$) [3]. Here $n_d = 2 - n_a$, and $\omega_{0_{a(d)}}$ and $E_{a(d)}$ are respectively plasmon frequencies and differences between upper and lower electron band for the acceptor (donor) sublattices. Furthermore, the multipole expansion can be performed for all Coulomb matrix elements except for the first neighbor short-range interaction V_{sr} in the \mathbf{a} direction. In the $\mathbf{q} \rightarrow 0$ limit we keep for three types of the Coulomb matrix elements present in eq.3, namely those with intraband-intraband, intraband-interband and interband-interband scatterings, the leading, i. e. monopole-monopole ($V_{0_e 0_f} = 4\pi e^2 / v_0 q^2$), monopole-dipole ($V_{0_e 1_f} = 4\pi i e \boldsymbol{\mu}_f \cdot \mathbf{q} / v_0 q^2$) and dipole-dipole ($V_{1_e 1_f} = 4\pi [3(\boldsymbol{\mu}_e \cdot \mathbf{q})(\boldsymbol{\mu}_f \cdot \mathbf{q}) - q^2 \boldsymbol{\mu}_e \cdot \boldsymbol{\mu}_f] / 3q^2 + V_{sr}$), contributions respectively. v_0 is the volume of the unit cell. Note that the difference between the longitudinal ($\mathbf{q} \parallel \mathbf{b}$) and transverse ($\mathbf{q} \perp \mathbf{b}$) dipole-dipole matrix elements, which will appear in the further analysis, is independent of \mathbf{q} , as well as of the details of the crystal structure [17], $V_{1_e 1_f, l} - V_{1_e 1_f, t} = (4\pi \mu_e \mu_f) / v_0$.

From the form of the matrix (3), one may already recognize the hybridizations which lead to collective modes. We start with the upper diagonal 2×2 block which represents intraband (metallic) polarizations with long range monopole-monopole interactions. They give rise to two plasmon modes, the hybrids of plasmons from acceptor and donor sublattices. For strictly one-dimensional electron bands, one of these hybridized modes is acoustic, while the other is optic, with a frequency which vanishes in the limit $\mathbf{q} \rightarrow 0$ for $\mathbf{q} \parallel \mathbf{b}$, and is equal to $\omega_0 = \sqrt{\omega_{0_a}^2 + \omega_{0_d}^2}$ for $\mathbf{q} \parallel \mathbf{b}$ [7].

The lower diagonal 2×2 block includes interband processes, which, due to finite dipole matrix elements at both types of molecules, induce long-range dipole-dipole interactions. The corresponding collective modes

$$\omega_{\pm}^2 = \frac{1}{2} \left[\omega_a^2 + \omega_d^2 \pm \sqrt{(\omega_a^2 - \omega_d^2)^2 + 16n_a n_d E_a E_d V_{1_a 1_d}^2} \right] \quad (4)$$

are hybrids of dipolar modes from two sublattices, $\omega_{a(d)}^2 = E_{a(d)} [E_{a(d)} + 2n_{a(d)} V_{1_{a(d)} 1_{a(d)}}]$. The frequencies of the dipolar modes decrease from $\omega_{i,l}$ to $\omega_{i,t}$ [$i \equiv a, d, \pm$] as the orientation of \mathbf{q} changes from $\mathbf{q} \parallel \mathbf{b}$ to $\mathbf{q} \perp \mathbf{b}$ [14] [and do not vary as \mathbf{q} rotates within the plane (\mathbf{a}, \mathbf{c})]. Note that the frequency differences $\omega_{i,l}^2 - \omega_{i,t}^2$ are, like the corresponding differences of dipole-dipole matrix elements, insensitive to the details of the crystal structure.

A further hybridization between plasmon ω_0 and longitudinal dipolar (4) modes takes place through the off-diagonal 2×2 blocks in the matrix (3). Due to the diverging long-range monopole-dipole Coulomb matrix elements, the latter do not vanish, provided the lower bands are metallic. The frequencies of the three new hybridized longitudinal modes are solutions of

the equation

$$\omega^2(\omega^2 - \omega_{-l}^2)(\omega^2 - \omega_{+l}^2) - \omega_0^2(\omega^2 - \omega_{-t}^2)(\omega^2 - \omega_{+t}^2) = 0, \quad (5)$$

which we denote by $\Omega_{1,2,3}$. Although the transverse dipolar frequencies $\omega_{\pm t}$ are not affected by the monopole-dipole interactions, they enter into eq. 5, in agreement with our general results for multiband metallic systems [14]. This has an important implication when ω_{-t} , the frequency of the lower transverse mode, is small, i. e. when

$$V_{1a1d,t} \approx \frac{\omega_{at}\omega_{dt}}{2\sqrt{n_a n_d E_a E_d}}, \quad (6)$$

which is, as we argue below, the case in TTF-TCNQ. Then Ω_1 , the frequency of the lowest longitudinal mode from eq. 5, is also small and lies below ω_{-t} , i. e.

$$\frac{\Omega_1^2}{\omega_{-t}^2} \approx \left[1 + \left(\frac{\omega_{-l}\omega_{+l}}{\omega_0\omega_{+t}} \right)^2 \right]^{-1}. \quad (7)$$

The frequencies $\omega_{a(d)t}$ are presumably comparable with the corresponding values in the homomolecular crystals of TCNQ and TTF molecules. Dielectric data for TCNQ crystals give $\omega_{at} \approx E_a$ [19]. Analogous data for TTF are not available, but, having in mind that the spectra of the TTF and TCNQ molecules are similar [16], [15], and that both homomolecular crystals have similar cohesion energies of 1eV [21], we expect that $\omega_{dt} \approx E_d$, too. Thus the condition (6) is physically equivalent to the requirement $E_a, E_d, V_{1a1d} \gg V_{1a1a}, V_{1d1d}$, which in particular means that the dipolar coupling between donor and acceptor sublattices is much stronger than that within each sublattice. Since this is not a property of the dipolar long-range lattice sums, i. e. the product of the long range parts of V_{1a1a} and V_{1d1d} is of the same order of magnitude as the square of the long range part of V_{1a1d} , the dominance of V_{1a1d} is to be sought in the details of the short-range contributions from nearest neighboring pairs of chains. We emphasize that, while the soft transverse mode ω_{-t} appears due to the strong, mainly local, dipolar fluctuations, the accompanying soft longitudinal mode Ω_1 from eq. 7 appears due to their coupling of long-range intraband fluctuations.

The macroscopic dielectric function which corresponds to the matrix (3) is given by [14]

$$\epsilon_M = \frac{(\omega^2 - \Omega_1^2)(\omega^2 - \Omega_2^2)(\omega^2 - \Omega_3^2)}{(\omega^2 - \omega_{-t}^2)(\omega^2 - \omega_{+t}^2)} \quad (8)$$

for $\mathbf{q} \parallel \mathbf{b}$, and $\epsilon_M = 1$ for $\mathbf{q} \perp \mathbf{b}$. Since these functions correspond to the optical (transverse) dielectric functions for the orientation of the electric field parallel and perpendicular to the chain direction respectively, we can make a link with experiments, keeping in mind that above expressions for ϵ_M do not contain contributions from interchain electron hoppings, molecular and lattice vibrations (including the $2k_F$ CDW collective modes), relaxation processes, etc. In particular, we assign the modes Ω_1 and ω_{-t} to the respective excitations at ~ 10 meV and ~ 57 meV, observed at 100 K in the infra-red measurements [10, 11], and the mode Ω_2 to the excitation at ~ 0.75 eV, originally interpreted as a Drude edge [9, 13] (fig. 1). The modes ω_{+t} and Ω_3 are most likely situated in the frequency range of few eVs, not investigated experimentally in detail and usually attributed to the range of interband transitions. It is noteworthy to mention in this respect a strong anomaly at ~ 4.5 eV observed in the early reflectivity data [9].

The two most interesting modes, denoted here by Ω_1 and ω_{-t} , invited various theoretical explanations. Here we list arguments in favor of the present one. First, our model predicts the optical activity in the chain \mathbf{b} direction, in agreement with experiments [10, 11], and in

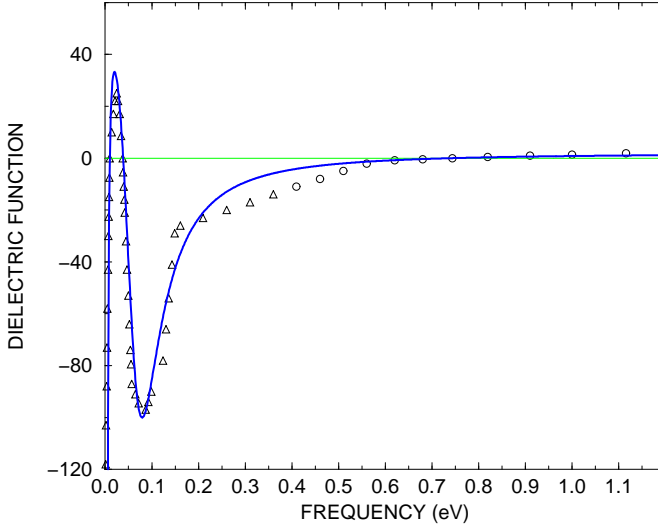


Fig. 1. – The real part of the dielectric function for TTF-TCNQ at 100 K with the data taken from Refs. [11] (triangles) and [10] (circles). The full line is $\text{Re } \epsilon_M$ (eq. 8) with the zeros at $\Omega_1 = 10 \text{ meV}$, $\Omega_2 = 750 \text{ meV}$, and $\Omega_3 = 6 \text{ eV}$, and poles at $\omega_{-t} = (57 + i42) \text{ meV}$ and $\omega_{+t} = 4.5 \text{ eV}$. The imaginary part in ω_{-t} is chosen to fit the experimental width of the pole in $\text{Re } \epsilon_M$.

contrast to the interpretation in terms of lattice vibrations [18]. The latter are optically active only when polarized along the transverse \mathbf{a} direction, in which the oppositely charged chains are aligned. Our suggestion that the regime (6) is appropriate for TTF-TCNQ is based on the observation that the frequencies Ω_1 , ω_{-t} , and Ω_2 are much lower than those of other modes from eq.8, which lie in the range of bare interband dipolar modes ($\sim 3 \text{ eV}$). Furthermore, the experimentally determined difference of $\sim 0.7 \text{ eV}$ between frequencies Ω_2 and ω_{-t} [10], which are the longitudinal and transverse edges of one hybridized branch (out of three), is comparable to the difference of $\sim 1.5 \text{ eV}$ between analogous frequencies in, e.g., the TCNQ crystal [19] (although the characteristic values of latter are of the order of a few eV). Since these differences measure the differences between longitudinal and transverse lattice sums in the matrix elements V_{11} , it follows that the long-range contribution in V_{1a1d} is comparable to those in V_{1a1a} and V_{1d1d} , in accordance with the already mentioned general result [14]. In other words, the small values of both ω_{-t} and Ω_2 may originate only from the short-range \mathbf{q} -independent part of V_{1a1d} , in agreement with our arguments below eq.7.

The onset of CDW order below $\sim 50K$, which causes the appearance of the well-known features in the far infra-red range due to the CDW dynamics [12], have also important effects on the modes of eq.8. At first, the low-lying longitudinal mode Ω_1 is eliminated [12, 13] due to the formation of the insulating gap Δ_L at the Fermi level, in agreement with our general predictions [14]. The modulation of the crystal structure in the insulating phase below the temperature of the Peierls phase transition also causes a weak splitting of remaining transverse and longitudinal modes [14], in analogy with Davydov splitting of molecular excitons [20]. Such splitting is indeed observed for the mode ω_{-t} at $\sim 50 \text{ meV}$ [13]. We expect that more refined measurements would show the same splitting for other modes, e.g. for the mode Ω_2 at 0.75 eV .

It remains to consider the contribution of the polarization modes (5) to the cohesion. Extending the standard RPA procedure to the present multi-band system, one arrives at

the cohesion energy per unit cell

$$E_{coh} = E_I n_a - E_M n_a^2 + \frac{1}{2N} \sum_{\mathbf{q},j} \omega_j(\mathbf{q}) - E_a - E_d, \quad (9)$$

where ω_j are hybridized modes from eqs.4,5. Due to the condition(6), the expression (9) reduces for $n_a \leq 1$ to

$$E_{coh} \approx -(2C - D - E_I)n_a + (C - \frac{A}{4} - \frac{D}{4} - E_M)n_a^2 - D, \quad (10)$$

Here $A(D) \equiv \sum_{\mathbf{q}} V_{1a(d)}^2 / 2NE_{a(d)}$, $C \equiv \sum_{\mathbf{q}} V_{1a1d}^2 / N(E_a + E_d)$, and E_I and E_M are affinity-ionicity and Madelung energy respectively. Noting that, in accordance with foregoing arguments, $A, D \ll C$, it follows from eq.10 that only with $2C - E_I > 0$ and $C - E_M > 0$ is partial charge transfer possible. In the case of TTF-TCNQ this means that, roughly, $C > 2\text{eV}$, which just compensates the "Madelung defect" on one side, and is consistent with the condition for the ω_{-t} mode softening (6) on the other. As was already pointed out, the dominant contribution to C is expected to come from the nearest-neighbor interaction V_{sr} between acceptor and donor pairs, i. e. from the **a** direction which is indeed the direction of smallest compressibility in TTF-TCNQ [4]. This interchain coupling is expected to be responsible for the fractional charge transfer in other OCCs as well. The fractional charge transfer is thus predicted to be relatively insensitive to the type of stacking in the **c** direction, which explains the similarity of the observed charge transfers in e. g. TTF-TCNQ and HMTTF-TCNQ.

Let us now turn our attention to the relative stability of TTF-TCNQ and HMTTF-TCNQ lattices. Note that the short-range contribution from nearest neighbors in the **a** direction to the sum C does not enter into the difference of corresponding cohesion energies (10), while the contributions to the sums A, D, C from the neighboring molecular pairs in the **c**-direction which now become relevant, can be represented in the Friedel dipole-dipole form. Taking for simplicity $n_a = 1$, we come to the condition that TTF-TCNQ lattice is more stable than the HMTTF-TCNQ lattice provided that

$$\left[\left(\frac{\mu_a^2}{\sqrt{E_a}} - \frac{\mu_d^2}{\sqrt{E_d}} \right)^2 + 2 \frac{\mu_a^2 \mu_d^2 (\sqrt{E_a} - \sqrt{E_d})^2}{\sqrt{E_a E_d} (E_a + E_d)} \right] \left(\frac{1}{c^6} - \frac{1}{[(a/2)^2 + c^2]^3} \right) \geq E_M(H) - E_M(T). \quad (11)$$

$E_M(H)$ and $E_M(T)$ are Madelung energies of HMTTF-TCNQ and TTF-TCNQ lattices respectively. The left-hand side of this expression amounts to the second order van der Waals contribution. It is a slight generalization of the original Friedel criterion, since $E_a \neq E_d$ and the contribution from the diagonal $\mathbf{a}/2 + \mathbf{c}$ direction is taken into account. We note that the characteristic energies which are responsible for the relative stability of TTF-TCNQ and HMTTF-TCNQ lattices are much smaller than those which determine the total cohesion, including the contributions from the coupling in the **a** direction which is decisive for the fractional charge transfer. Indeed, the simple calculations of the differences of the Madelung [7] and the van der Walls energies in the point charge approximation by using the numerical values for the molecular polarizabilities [22, 23], suggest that both differences are of the order of 0.1eV per unit cell.

In summary, we have shown that the interband collective modes are responsible for the crystal stability of OCCs, while the hybridization of these modes with intraband plasmons explains the low frequency optical data in TTF-TCNQ in particular. We argue, and this is the crucial point of our model, that the frequencies of three collective modes are rather low, i.e. below 1 eV. It is worthy to note that, since one of them falls into the frequency range of the CDW instabilities (≤ 10 meV), we are confronted with the interesting possibility of a

mixing of these two types of correlation at low temperatures. This question is left for future investigations. Clearly, the concepts developed and successfully used here can also be applied to the other metallic systems with large molecular polarizabilities.

Acknowledgments: We acknowledge the valuable remarks of J. Friedel.

REFERENCES

- [1] S. BARIŠIĆ and A. BJELIŠ, in *Electronic properties of organic materials with quasi-one-dimensional structure*, edited by KAMIMURA H., (Riedel Publ. Comp., New York, Dordrecht, 1985 p. 49.
- [2] R. M. METZGER and A. N. BLOCH, *J. Chem. Phys.*, **63** (1975) 5098.
- [3] A. J. EPSTEIN *et al.*, *Phys. Rev.*, **B13** (1976) 1569.
- [4] D. DEBRAY *et al.*, *J. Physique Lett.*, **38** (1977) L-227.
- [5] V. E. KLYMENKO *et al.*, *Zh. Eksp. Teor. Fiz.*, **69**, (1975) 240. [Sov. Phys. JETP **42**, 123 (1976)]; J. B. TORRANCE and B. D. SILVERMAN, *Phys. Rev.*, **B15** (1977) 788.
- [6] R. M. METZGER, *J. Chem. Phys.*, **75** (1981) 3087.
- [7] S. BARIŠIĆ and A. BJELIŠ, *J. Physique Lett.*, **44** (1983) L-327. P. ŽUPANOVIĆ *et al.*, *J. Physique*, **46** (1985) 1751.
- [8] J. FRIEDEL, in *Electron Phonon Interactions and Phase Transitions*, edited by T. RISTE, NATO Advanced Study Institute, Series B Physics (Plenum, New York) 1977.
- [9] P. M. GRANT *et al.*, *Phys. Rev. Lett.*, **31** (1973) 1311; A. A. BRIGHT *et al.*, *Phys. Rev.*, **B10** (1974) 1328.
- [10] D. B. TANNER *et al.*, *Phys. Rev.*, **B13** (1976) 3381.
- [11] C. S. JACOBSEN, in *Lecture Notes in Physics*, Vol. **95** edited by S. BARIŠIĆ *et al.*, (Springer-Verlag, Berlin) 1979 p. 223.
- [12] D. B. TANNER *et al.*, *Phys. Rev. Lett.*, **47** (1981) 597 ; J. E. ELDRIGE and E. BATES, *Phys. Rev.*, **B28** (1983) 6972; J. E. ELDRIGE, *Phys. Rev.*, **B31** (1985) 5465.
- [13] H. BASISTA *et al.*, *Phys. Rev.*, **B42** (1990) 4088.
- [14] P. ŽUPANOVIĆ *et al.*, *Z. Phys.*, **B97** (1995) 113 ; *ibid* **B101** (1996) 387, 397.
- [15] D. A. LOWITZ, *J. Chem. Phys.*, **46** (1967) 4698.
- [16] B. I. BENNETT and F. HERMAN, *Chem. Phys. Lett.*, **32** (1975) 334 .
- [17] M. H. COHEN and F. KELLER, *Phys. Rev.*, **99** (1955) 1128.
- [18] L. P. GOR'KOV and E. I. RASHBA, *Sol. State Commun.*, **27** (1978) 1211.
- [19] R.R. PENNELLY and C.J. ECHARDT, *Chem. Phys.*, **12** (1976) 89 .
- [20] A. S. DAVYDOV, in *Theory of Molecular Excitons*, (Plenum Press, New York) 1971.
- [21] C.G. DE KRUIF and H.A.J. GOVERS, *J. Chem. Phys.*, **73** (1980) 553.
- [22] V.E. KLYMENKO, *Ukrainskii Fizicheskii Zhurnal*, **23** (1978) 1301.
- [23] M.A. RATNER, *Chem. Phys. Letters*, **28** (1974) 383.